Available online at www.sciencedirect.com
SCIENCE DIRECT®
Journal of Hydrology 316 (2006) 53–70
Journal of Hydrology
www.elsevier.com/locate/jhydrol

Hydroclimatology of the North American Monsoon region in northwest Mexico

David J. Gochis[a,*], Luis Brito-Castillo[b], W. James Shuttleworth[c]

[a]National Center for Atmospheric Research[1], P.O. Box 3000, Boulder, CO 80307-3000, USA
[b]Centro de Investigaciones Biologicas del Noroeste (CIBNOR), Guaymas, Sonora, Mexico
[c]Department of Hydrology and Water Resources, University of Arizona, Tucson, AZ, USA

Received 1 November 2004; revised 7 April 2005; accepted 27 April 2005

Abstract

The North American Monsoon (NAM) system controls the warm season climate over much of southwestern North America. In this semi-arid environment, understanding the regional behavior of the hydroclimatology and its associated modes of variability is critically important to effectively predicting and managing perpetually stressed regional water resources. Equally as important is understanding the relationships through which warm season precipitation is converted into streamflow. This work explores the hydroclimatology of northwestern Mexico, i.e. the core region of the NAM, by (a) presenting a thorough review of recent hydroclimatic investigations from the region and (b) developing a detailed hydroclimatology of 15, unregulated, headwater basins along the Sierra Madre Occidental mountains in western Mexico. The present work is distinct from previous studies as it focuses on the intra-seasonal evolution of rainfall-runoff relationships, and contrasts the sub-regional behavior of the rainfall-runoff response. It is found that there is substantial sub-regional coherence in the hydrological response to monsoon precipitation. Three physically plausible regions emerge from a rotated Principal Components Analysis of streamflow and basin-averaged precipitation. Month-to-month streamflow persistence, rainfall-runoff correlation scores and runoff coefficient values demonstrate regional coherence and are generally consistent with what is currently known about sub-regional aspects of NAM precipitation character.

Keywords: North American Monsoon; Hydroclimate; Runoff; Regionalization; Intra-seasonal variability; Mexico

1. Introduction

An increasing body of literature is documenting salient features of the North American warm-season circulation and precipitation regime over the region of northwestern Mexico that is the core of the North American Monsoon System (NAMS). The region is generally semi-arid, with an annual precipitation regime dominated by warm-season convection that strongly interacts with the regional topography and surrounding bodies of seawater (For a complete discussion of the NAMS, please refer to the North American Monsoon Experiment (NAME) Science

* Corresponding author.
E-mail address: gochis@rap.ucar.edu (D.J. Gochis).
[1] The National Center for Atmospheric Research is sponsored by the National Science Foundation.

0022-1694/$ - see front matter © 2005 Elsevier B.V. All rights reserved.
doi:10.1016/j.jhydrol.2005.04.021

Plan (NAME Science Working Group, 2004) or Higgins et al., 2003). The circulation features responsible for this warm-season precipitation regime have been well documented (Higgins et al., 1997; 1998; 1999; Higgins and Shi, 2000; Carleton et al., 1990; Douglas et al., 1993; Schmitz and Mullen, 1996; Castro et al., 2001; Hu and Feng, 2002). Such studies consistently document a transition in the regional climate from an arid subtropical regime dominated by westerly flow at middle and upper levels, to a regime with substantially higher relative humidity, easterly flow at mid and upper levels, and strong diurnal convection. This transition occurs during June and early July and is designated as the 'onset' of the summer monsoon. The monsoon circulation, its onset, precipitation character, and the hydrological response to it, exhibit considerable spatial and temporal variability. This variability complicates diagnostic and predictive efforts and limits responsive management of regional water resources. This work explores the complex relationship between precipitation and streamflow in the NAM region by: (a) reviewing recent works that have examined precipitation and streamflow variability and (b) constructing a regional hydroclimatology from selected headwater catchments in northwest Mexico.

2. Background

2.1. Overview of the North American Monsoon precipitation regime

The internal structure of NAM precipitation is complex and subject to considerable spatial and temporal variability. The centroid of NAM precipitation, which is often defined as the total rainfall in July, August, and September (JAS), is located along the western slope of the Sierra Madre Occidental (SMO) in northwestern Mexico (Douglas et al., 1993; Higgins et al., 1999; Gochis et al., 2004). In this region, the coefficient of variation of precipitation is high in the global context (Dettinger and Diaz, 2000), but comparatively low relative to surrounding regions (Higgins et al., 1997; Mosino and Garcia, 1974). The region was identified as the leading pattern in a regionalization analysis of the warm-season precipitation regime for southwestern North America (Comrie and Glenn, 1998). Strong diurnal pulsing of low-level moisture flux helps drive the diurnal precipitation regime. Berbery (2001), Anderson et al. (2000), Stensrud et al. (1995), Gochis et al. (2003a; 2004) and Fawcett et al. (2002) have each documented distinct diurnal cycles in precipitation and low-level moisture fluxes over the Gulf of California and SMO. Here, precipitation is typically generated by deep convection that is initiated over the high terrain of the SMO and then propagates away, both eastward and westward, from the cordillera during the evening hours (e.g. Negri et al., 1994; Vazquez, 1999; Fawcett et al., 2002; Gochis et al., 2004). Precipitation in areas peripheral to this 'core' monsoon region exhibit high spatial and temporal variability, and precipitation appears to be closely dependent on transient features such as the passage of mid-latitude waves, tropical easterly waves (Fuller and Stensrud, 2000), and, very importantly, tropical storms (Douglas, 2000).

The NAM precipitation regime exhibits substantial variability on interannual to interdecadal timescales that is potentially linked via teleconnections to remote forcing. Variability on these timescales can be critically important for the effective management of water resources (e.g. Brito-Castillo et al., 2002). Sea surface temperatures (SSTs) in the North Pacific (e.g. Higgins and Shi, 2000; Englehart and Douglas, 2002; Brito-Castillo et al., 2002) and in the Gulf of California (Mo and Juang, 2003) each are somewhat correlated with NAM rainfall. Correlation structures display sub-regional spatial coherence such that particular SST anomalies are related to rainfall variability over specific regions within the core NAM region. For instance, using teleconnective correlation analyses, Englehart and Douglas (2002) showed that the region west of the SMO is modestly correlated with El Niño/Southern Oscillation (ENSO), but only during positive phases of the Pacific Decadal Oscillation (PDO). Conversely, during positive PDO phases, the altiplano or plateau region of central Mexico are not correlated with ENSO. Significant correlation between ENSO and precipitation during the negative phase of the PDO are not found in either region.

Englehart and Douglas also show that rainfall in both of these regions appears to be related to the positioning of the subtropical anticyclone. In particular, rainfall in the western SMO is weakly positively

correlated with a northward-displaced ridge during positive phases of the PDO, while precipitation in the altiplano region is strongly negatively correlated with a northeastward-displaced ridge during negative phases of the PDO. A clear understanding of how the combined effects of ENSO and PDO modulated the anticyclone position, however, was not provided. During periods when there is significant teleconnection between remote-ocean forcing and NAM precipitation, there is the potential for responsive water resources management in this region, but only if the streamflow response to known or expected precipitation characteristics is well understood.

2.2. Streamflow under the North American Monsoon

Available studies of streamflow in the NAM region suggest that the regional streamflow regime is similar to that of other subtropical, semi-arid monsoon systems elsewhere in the world (Descroix et al., 2002a,b). Using a large-scale cluster analysis, Dettinger and Diaz (2000) showed that hydrological systems in the NAM region are characterized by a late summer peak in the monthly fraction of annual streamflow, and that they provide the link in the latitudinal transition between snowmelt-dominated streamflow further north and tropical streamflow regimes further south. On interannual and longer time scales, NAM streamflow has been linked to both the ENSO (Magaña, 1999; Magaña and Conde, 2000) and the PDO (Brito-Castillo et al., 2002). Corresponding to long-term variability in precipitation, relationships between SST and streamflow exhibit both constructive and deconstructive tendencies, such that different combinations of ENSO and PDO phases can be related to either increases or decreases in regional streamflow volume. There is evidence that teleconnections exist between Pacific SSTs and streamflow in NAM river systems, but the correlation values are modest and appear to vary with the selected climatological period for which analysis is made (Brito-Castillo et al., 2002; 2003).

Only recently have there been attempts to regionalize streamflow behavior across the core NAM region (e.g. Brito-Castillo et al., 2002; 2003). Brito-Castillo et al. (2002) constructed regional diagnostics using calculated monthly inflow volumes (MIV's) to reservoirs along mainstem river systems draining the western slope of the SMO. In general, elucidation of the 'natural' streamflow regime can be complicated using reservoir inflow data due to required assumptions concerning reservoir evaporation and seepage, inflow estimation errors as well as the presence of upstream operations, which can include impoundments and/or diversions. Nevertheless, the analyses in Brito-Castillo et al. (2002), and, subsequently, in Brito-Castillo et al. (2003), provide a preliminary understanding of a general hydrologic regime in western Mexico. Using a rotated principal components analysis, it was found that July–August–September MIV (Brito-Castillo et al., 2002) and streamflow (Brito-Castillo et al., 2003) along the western SMO broadly cluster into two significant regions of spatial coherence; a northern region and a southern region. The northern region encompasses the river systems emanating from the northern SMO, a region typified, in the summertime, by large mesoscale convective storms, which occur, comparatively, less frequently than convection further south (Gochis et al., 2004). The southern region encompasses river systems draining the western SMO with headwaters in western Durango and eastern Sinaloa. Composite analyses of wet and dry years revealed that positioning of the summertime 700 mb ridge can be important for establishing sustained moisture transport into the various regions underlying the NAM (Brito-Castillo et al., 2003).

Dettinger and Diaz (2000) showed that the interannual variance of streamflow in the southwestern US and western Mexico is among the highest in the world and is higher than that of precipitation. This feature suggests a non-linear response of streamflow to precipitation forcing. Consequently, a clear understanding of physical processes will be required to predict streamflow from precipitation forecasts. In fact, the modeling study by Gochis et al. (2003a) suggests that surface runoff may be better correlated with specific features of the NAM precipitation regime, such as intensity and duration of discrete storms, than with basin-averaged or time-average rainfall.

Annual values of the runoff coefficient, defined as the volume of runoff divided by the volume of precipitation, have been estimated to be between 0 and 20% within the state of Sonora (INEGI, 1993) and between 0 and 30% within the state of Sinaloa

(INEGI, 1995). However, to date, no comprehensive study has been made of how the warm season rainfall-runoff response is affected by the spatio-temporal characteristics of precipitation across the NAM region, in general, and in northwest Mexico, in particular. Critical information on rainfall statistics from storm to seasonal time scales and important information on watershed characteristics are only recently becoming available (e.g. Gochis et al., 2004). The current lack of precipitation data with temporal resolution sufficient to resolve the diurnal cycle of rainfall intensity translates into a lack of understanding of the critical processes responsible for generating streamflow in the NAM region and, ultimately, of how the water resources in this region might respond to interannual to interdecadal climate variability.

2.3. Plot to catchment scale studies

Hydrological processes operating at smaller (catchment) scales show a strong dependence on features of the NAM precipitation regime as well as local physiographic features. Michaud et al. (2000) demonstrated that small-basin floods in the southwestern US are generated by short-duration ($\sim$0.5–1.0 h), high-intensity (10–100 mm/h) convective storms during the warm season. Streamflow from these storms is therefore likely generated by the Hortonian (or infiltration excess) mechanism rather than by saturation excess. Descroix et al. (2002a) also found that runoff in the SMO region was generated by the Hortonian mechanism but, interestingly, also exhibited threshold responses to seasonal total precipitation amounts. High evaporation rates and the generally low antecedent precipitation (and hence low antecedent soil moisture) were hypothesized to inhibit complete saturation of soil profiles, thereby reducing the size of contributing source areas of overland flow or the generation of sustained baseflow. Thin soils and steep, complex terrain are also believed to contribute to the generation of small-basin floods in this region (Michaud et al., 2000). In an intensely studied site in northwestern Durango (on the east slope of the SMO), Descroix et al. (2002b) found that approximately 85% of hillslope soils exhibited soil depths between 10 and 60 cm.

Under heavy to extreme precipitation events, rainfall intensities determine the partitioning of effective precipitation between water that infiltrates the soil and water that becomes overland runoff. Descroix et al. (2002b) showed that, at lighter rainfall intensities, soil characteristics become increasingly important. Factors affecting the infiltration of light to moderate precipitation intensity events include hydraulic conductivity, the presence of soil crusts, percent of stone coverage and the structure or layering of soil elements. One of the primary findings of Descroix et al. (2002b) was that hydraulic conductivity values were found to be *uncorrelated* with soil structural and texture data. Their results showed that 70% of the total variability in hydraulic conductivity values calculated within a 400 km^2 area can also be observed within 4 km^2. It was suggested that hydraulic conductivity values may be better correlated with terrain slope values, percent stone cover and vegetation cover than with soil texture.

Additionally, Viramontes and Descroix (2003), analyzing the changing character of hydrograph response from two catchments along the eastern flank of the SMO, found that significant alterations in landscape characteristics are currently impacting runoff genesis. Specifically, basin lag times, streamflow contributions from baseflow, and flood hydrograph recession times all decreased from the 1970s to the 1990s. Lacking long-term trends in rainfall or runoff volume, they concluded that changes in hydrograph response were primarily landscape-driven and not climate driven. Taken together, these findings complicate the task of developing and implementing either statistically or physically based hydrological models for streamflow and water resources prediction.

2.4. Outline

In this paper, we extend several of the existing works discussed above by analyzing observed streamflow and gridded precipitation records for 15 unregulated basins situated along the cordillera of the SMO underlying the core of the NAMS. As such, the work presented below constitutes a regional hydroclimatology of basins draining the mountains in northwest Mexico based on currently available data. The motivation for this effort is two-fold; the first is to create a comprehensive documentation of

principal hydroclimatic features within the core region of the North American Monsoon. The second motivation is to elucidate the evolution of rainfall-runoff relationships throughout the monsoon season, which may have predictive value in the context of hydrological forecasts from the daily to seasonal timescales. Section 3 outlines the data and procedures used in this study. Seasonal streamflow characteristics, streamflow regionalization, lagged autocorrelation analyses, rainfall-runoff correlation and runoff coefficient analyses are all presented in Section 4. Conclusions and summary remarks are presented in Section 5.

3. Data and methods

3.1. Data

Selected basins, pertinent basin characteristics and streamgauge locations are shown in Fig. 1 and listed in Table 1. Monthly streamflow data were obtained from the BANDAS (Banco Nacional de Datos de Aguas Superficiales) data archive, BANDAS (1998). This data set is jointly developed by the Comision Nacional del Agua (CNA) and the Instituto Mexicano de Tecnologia del Agua (IMTA) of Mexico, and is continually updated. Streamflow periods of record vary for individual basins, but all basins possess at least 10 years of data. Similar to Brito-Castillo et al. (2003), we have chosen to use observed streamflow from headwater catchments, which are, to the best of the authors' knowledge, unregulated. Most of these catchments lay in remote areas in the higher terrain of the SMO. The size of the catchments studied in the present analysis ranges from 1000 to 10,000 km^2 while those used in Brito-Castillo ranged between 223 and 26,000 km^2. Thus, the results presented herein are more constrained to focus on the 'natural' hydrological response of typical SMO headwater catchments to monsoon rains. Three of the 15 basins studied (Table 1; 1. Rio San Pedro del Conchos, 7. Rio Sextin, and 11. Rio Ramos) drain to the east of the North American cordillera towards the Mexican Plateau whereas Brito-Castillo et al. (2003) only focused on western SMO basins. Additionally, in the present work, emphasis is placed on examining the intraseasonal evolution of monthly streamflow, as opposed to strictly focusing on aspects of the interannual variability of streamflow. Given these differences, the present analysis should be viewed as a logical expansion of that given by Brito-Castillo et al. (2003), which extends depiction of the regional hydrological regime to both sides of the SMO and to the intra-seasonal timescale.

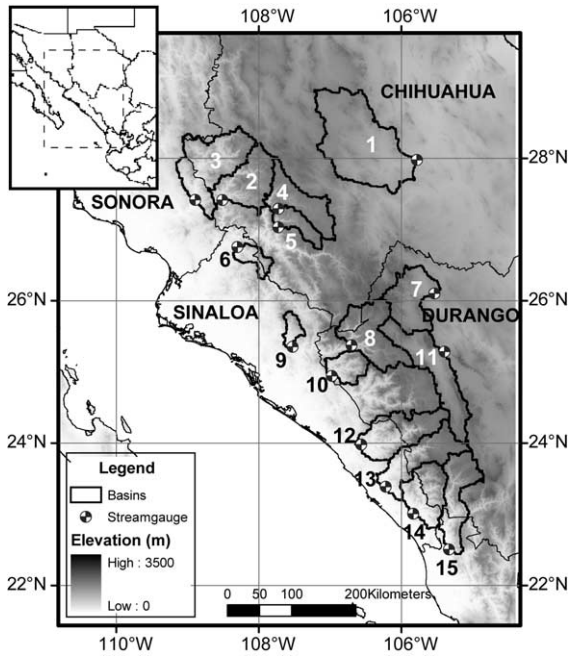

Fig. 1. Map of selected headwater basins in northwest Mexico. Inset shows the larger region surrounding the Gulf of California. Topography is in grey-shading.

Rainfall data used in these analyses was from the 1948–1998, daily, 1° gridded precipitation dataset for Mexico, of Higgins et al. (1996). This dataset has been used extensively for numerous long-term studies of Mexican rainfall variability (e.g. Higgins and Shi, 2000; 2001; Higgins et al., 1999; Mo and Peagle, 2000). Basin average precipitation for each basin was calculated by averaging grid values contained within each individual basin using the ARC/INFO (ESRI, 2003) spatial statistics functions, as was done by Gochis et al. (2003a). There are several issues that are raised when using a gridded dataset of 1° horizontal resolution for this kind of analysis. First, the gridded dataset is generated using a modified Cressman analysis (Cressman, 1959) of daily climate station observations. This procedure inherently smoothes the

Table 1
Listing of 15 headwater basins from northwest Mexico and selected basin attributes

Station	River	Drainage basin	Drainage area (km^2)	Gage location (deg)	Gage location (deg)	Period of record	Mean annual flow volume (10^3 m^3)	Annual coefficient of variation
1. Villalba*	San Pedro del Conchos	Conchos*	9405	−105 46 40	27 59 10	1938–90	411401	0.637
2. Chinipas	Chinipas/ Oteros	Fuerte	5098	−108 32 30	27 25 00	1965–98	1023985	0.505
3. San Bernardo	Mayo	Mayo	7510	−108 52 55	27 24 45	1960–99	1003542	0.401
4. Urique	Urique	Fuerte	4000	−107 50 20	27 18 10	1968–99	439165	0.546
5. Batopilas	Batopilas	Fuerte	2033	−107 44 15	27 01 20	1982–97	372859	0.383
6. Choix	Choix	Fuerte	1403	−108 19 45	26 44 10	1955–98	295679	0.374
7. Sardinas*	Sextin or del Oro*	Aguanaval*	4911	−105 34 12	26 05 00	1970–94	524074	0.610
8. La Huerta	Humaya	Culiacan	6149	−106 42 00	25 22 10	1969–99	1120591	0.502
9. Badiraguato	Badiraguato	Culiacan	1018	−107 32 15	25 20 00	1959–99	252900	0.611
10. Tamazula	Tamazula	Culiacan	2241	−106 58 30	24 56 00	1962–99	648172	0.348
11. Salome Acosta*	Ramos*	Aguanaval*	7130	−105 24 52	25 16 06	1969–94	557191	0.474
12. Ixpalino	Piaxtla	Piaxtla	6166	−106 35 45	23 57 20	1952–99	1627005	0.359
13. Siquerios	Presidio	Presidio	5614	−106 15 00	23 00 30	1956–99	1044081	0.518
14. Baluarte II	Baluarte	Baluarte	4635	−105 50 30	22 59 00	1947–99	1774999	0.422
15. Acaponeta	Acaponeta	Acaponeta	5092	−105 20 30	22 29 00	1945–99	1362309	0.382

Basins draining to the east of the SMO are indicated with an asterisk (*).

precipitation field and will inevitably produce erroneous values in regions where observations are sparse and terrain is complex, such as in the high terrain of the SMO. Based on limited data comparison with the NAME Event Raingauge Network (NERN) described by Gochis et al. (2003b; 2004), the effect of this smoothing is to: (a) overestimate the frequency of precipitation for a given point, (b) underestimate precipitation in a core region along the axis of the SMO, and (c) to overestimate precipitation in regions peripheral to the core region. Due to the limited duration of the NERN dataset, it is not yet clear what the implications of these biases are on monthly to seasonal totals. Second, a few of the basins are small compared to the effective grid size of the precipitation dataset. To account for this we resampled the 1° grid to 0.10° without additional smoothing or interpolation. This technique simply results in additional pixels for areal weighting of basin average precipitation estimates in those basins that straddle two or more 1° gridcells. Finally, all of the basins analyzed possess raingauges either within or directly adjacent to their watershed boundaries (e.g. at the watershed outlet). So although the gridded product possess significant, yet quantitatively unknown, biases due to smoothing in the analysis, the values are somewhat constrained by within-basin and/or nearby observed values. While use of this precipitation dataset is not ideal for fine spatial-scale hydrological analyses, it represents a practical compromise between the data needs for the analyses and those that are available and compatible with the intended analyses.

3.2. Methods

Various analyses were performed in order to define the regional hydroclimatological response to precipitation along the SMO in northwest Mexico. The annual cycle of streamflow for all the test basins is described below in terms of the monthly percentages of annual flow. Interannual variability of monthly streamflow is shown by plots of the monthly coefficients of variation[2]. Monthly maximum flow volumes are also plotted in order to illustrate

[2] The 'coefficient of variation' is defined here as the long term standard deviation of monthly streamflow volume divided by the long term monthly mean streamflow volume.

the annual cycle of maximum flows as well as some mechanistic causes for extreme events. The monthly, lag-1 ranked autocorrelation values are calculated for each of the river basins. These values, displayed on the annual cycle, show when month-to-month correlations in streamflow are high and can possibly be used to define periods of persistence predictability.

To examine regional coherence of streamflow and precipitation in the core NAM region, an empirical orthogonal function (EOF) analysis, similar to that of Brito-Castillo et al. (2002; 2003) and Comrie and Glenn (1998), was performed. Seasonal time series of streamflow and precipitation anomalies for July–August–September (JAS) were constructed. Due to differing periods of record, the streamflow time series were not strictly overlapping, and included occasions of missing data. Data from all basins were then decomposed in an EOF analysis using pairwise deletion of missing data from the correlation matrix. The degeneracy criteria of North et al. (1982) were applied to the un-rotated components in an attempt to determine which of the leading EOFs should be retained for analysis. In contrast to Brito-Castillo et al. (2002; 2003), use of these criteria resulted in the retention of greater than five components for both streamflow and precipitation variability. Varimax rotation (where, gamma = 1.0) was applied to all of components. The rotated loading factors of the retained components for streamflow and precipitation for each basin were plotted on a map at locations corresponding to basin stream gauging stations. Mapped station values were spatially interpolated using a simple inverse distance weighting algorithm, and smoothed using a low pass filter. Regional composites were created by retaining basins with EOF loading factors of greater than 0.6. The loading factor criterion of 0.6, obtained iteratively, ensured that all basins retained for each of the three regional composites contained statistically significant Spearman rank correlation values of their JAS streamflow anomalies at the 99% level.

For the present analysis, only the top three principal components of streamflow variability were retained. As discussed in Section 4.2, these regions represent physically plausible delineations of streamflow coherence, and explain more than 70% of the total sample variance. The remaining components of streamflow variability did not delineate well-defined regions. For precipitation, the three leading components explained approximately 86% of the total sample variance. A fourth principal component of JAS precipitation was found to be spatially coherent but was not explored extensively in the present work.

The relationships between monthly and seasonal rainfall and streamflow were evaluated from the lag-0 precipitation (P)-streamflow (Q) correlation and from the runoff coefficient (Q_r). Spearman rank correlation values were used, as opposed to Pearson values, because the Spearman rank value is less influenced by outliers than is the Pearson value. Lag-0, P–Q correlation values are presented here, as they possess substantially higher correlation values compared to lag-1 P–Q correlation values (not shown). While monthly rains do impact streamflow in the following month(s), given the small sizes of the basins studied (e.g. 1000–10,000 km^2), it was assumed that the principal hydrological response would have a lag time of shorter than 1 month. Here, Q_r is expressed as streamflow volume divided by total precipitation [i.e. $Q_r = Q/P$]. Effectively, Q_r describes the bulk fraction of rainfall that ends up as streamflow. This value can be influenced by basin size, and can also be related to the spatial distribution and intensity of rainfall, depending upon runoff generation mechanisms (e.g. infiltration excess vs. saturation excess). As will be shown below, this value can exhibit a large range over the course of a season.

4. Results

4.1. Streamflow climatology

The annual cycle of standardized monthly average flow volumes, monthly coefficients of variation and standardized monthly maximum flow volumes are shown in Fig. 2. Depending on the basin, 50–85% of the annual streamflow volume occurs during the months of July, August and September. Monthly streamflow volumes begin increasing in July and peak in either August or September. Notably, basins on the eastern slope of the SMO (shown in green) exhibit higher monthly percentages of annual streamflow volume during August and September, compared to the westward-draining basins. Monthly percentages of streamflow volume for October, for all basins, are

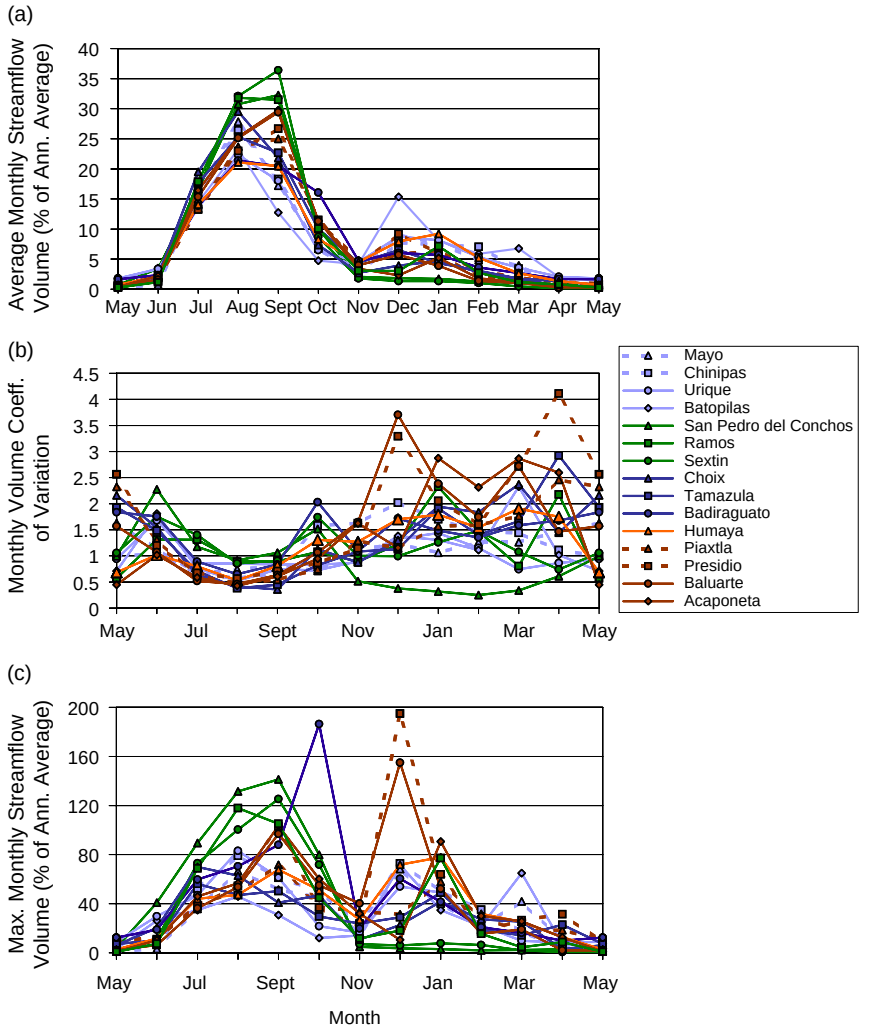

Fig. 2. (a) Normalized monthly average streamflow volumes, (b) coefficient of variation of monthly flow volumes, (c) normalized monthly maximum flow volumes.

comparable, though somewhat less, than those for July. Many basins exhibit small secondary peaks during December or January. These late-year, secondary peaks are likely due to the passage of slow-moving baroclinic disturbances that can drop large amounts of non-convective rainfall over the SMO during December and January.

Fig. 2(b) shows the coefficient of variation in monthly streamflow volume for each of the 15 basins. This plot identifies two distinct seasons in monthly streamflow variability. First, the primary monsoon months are characterized by comparatively low interannual variability. Typical standard deviations in streamflow between July and September are between 40 and 150% of their mean values. However, in absolute terms, monthly standard deviations are generally highest during the summer and fall months. Warm season monthly standard deviations of streamflow volume (not shown) range between 5 and 35% of the mean annual flow for all basins.

The second season of streamflow variability contains the remaining months (Oct–Jun) and is characterized by higher values of the coefficient of variation. For most basins, standard deviations range

between 75 and 350% of the mean monthly streamflow volume. (One noticeable exception to this pattern is the San Pedro del Conchos, which is discussed below.) The greater range of values among basins for non-monsoon months is indicative of increased variability in precipitation events. Although there is increased variability with respect to the mean monthly flow volumes in the non-monsoon months, these months constitute comparatively small fractions of the annual streamflow volume and, thus, of water resources. For instance, between March and May, monthly standard deviations (not shown) for nearly all basins are less than 10% of the mean annual flow.

Fig. 2(c) shows the annual cycle of monthly flow maximums normalized by the long term mean annual flow. While Fig. 2(c) highlights months which have experienced large events, it should be remembered that the periods of record from the basins do not strictly overlap. As in Fig. 2(b), there evidence of late fall and early winter streamflow variability shown in Fig. 2(c), where several basins in the southernmost region (e.g. Presidio, Baluarte, Humaya) have their peak, normalized, monthly maximum flows in December or January. Similar to Fig. 2(a), eastern slope basins have strong peaks in their maximum flow volumes during the summer. Of these eastslope basins only the Ramos basin shows the occurrence of a large flow event during the winter while both the Sextin and San Pedro del Conchos exhibit no large magnitude cold-season flows over their respective periods of record. Most of the other basins, residing in the central and northern SMO and in the western foothills, exhibit monthly maximum streamflow volumes during July and August, along with comparable secondary peaks during November and December. This feature is indicative of the dual regime discussed above, where large flows are generated by regular, seasonal monsoon rains or by lower frequency cool season events such as baroclinic systems.

As noted above, the San Pedro del Conchos maintains a persistently low value of the coefficient of variation from Nov to May. Fig. 2(c), indicates that there have been no large streamflow events recorded during these months over the period of record, which is 52 years. This unique behavior may be an indication of some type of human control of the river system, but to the authors' knowledge there are no large control structures above the streamflow observation point. If a large diversion project or control structure had been erected during the period of record, changes in the cumulative basin discharge (i.e. mass curve), keyed to a specific year, might be detectable. To explore the possibility of such influences further, a homogeneity analysis of streamflow from the San Pedro del Conchos was performed using the method detailed in Brito-Castillo et al. (1999). The homogeneity analysis (not shown) revealed low frequency (interdecadal) variations of annual and summer streamflow of the San Pedro del Conchos River that are superimposed on top of interannual variations. It could not be concluded from the homogeneity analysis that sub-samples of summer or annual flows from the entire period of record were distinguishable from a single full-record population. In effect, periodic shifts in multi-year average streamflow were not statistically different from each other or the entire sample mean. While the analysis was not exhaustive, it showed that the long-term shifts in the streamflow of the San Pedro del Conchos River at the Villalba gage station are likely attributable to low-frequency (i.e. decadal) climate variability. However, it is possible that small incremental implementations of control structures might not be significant enough individually to be detectable by the analysis conducted. Further exploration of the interaction of low- (interdecadal) and high-frequency (intra-seasonal to interannual) variability in winter and summer streamflows from the San Pedro del Conchos and other catchments in the NAM region is ongoing.

4.2. Regionalization of streamflow and precipitation

The EOF of JAS streamflow anomalies revealed three significant geographic regions of coherent streamflow-volume variability. The shared streamflow variations in these three basins explain approximately 71% of the total variance in JAS streamflow volume (25.4, 22.4, 23.1% for 'EOF1', 'EOF2' and 'EOF3', respectively). From the spatially interpolated loading factors plotted in Fig. 3(a)–(c), it can be seen that the leading components summarize variations in a north-central region (EOF1—Fig. 3(a); basins Mayo(3), Chinipas(2), Urique(4), and Humaya(8)), a southern region (EOF2—Fig. 3(b); basins Piaxtla(12), Presidio(13), Baluarte(14) and Acaponeta(15) and an eastern region (EOF3—Fig. 3(c); basins Sextin(7),

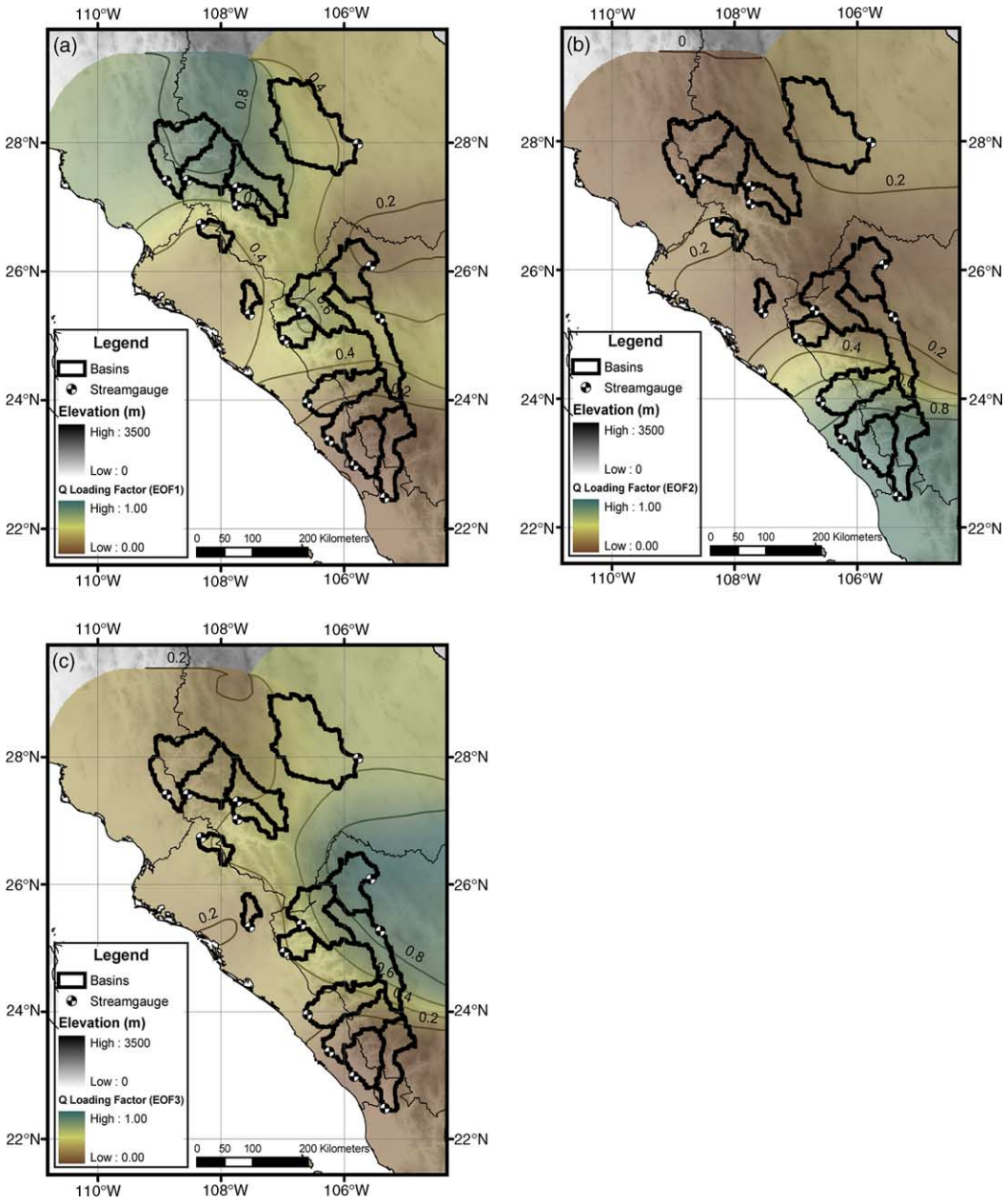

Fig. 3. Interpolated loading factors from PCA analysis of JAS streamflow for: (a) EOF1, (b) EOF2, and (c) EOF3. Contour interval is 0.2.

Ramos(11) and Batopilas(5)). These spatial patterns of streamflow variability are generally consistent with those of Brito-Castillo et al. (2002), although some of the details are different. The differences are likely due to the fact that this analysis included basins from the eastern slope of the SMO.

The interpolated loading factors for the first three principal components of JAS precipitation are shown in Fig. 4. Similar to streamflow, three coherent regions emerged: a northern region (EOF1—Fig. 4(a), which explained 45.1% of the total variance), a southern region (EOF2—Fig. 4(b),

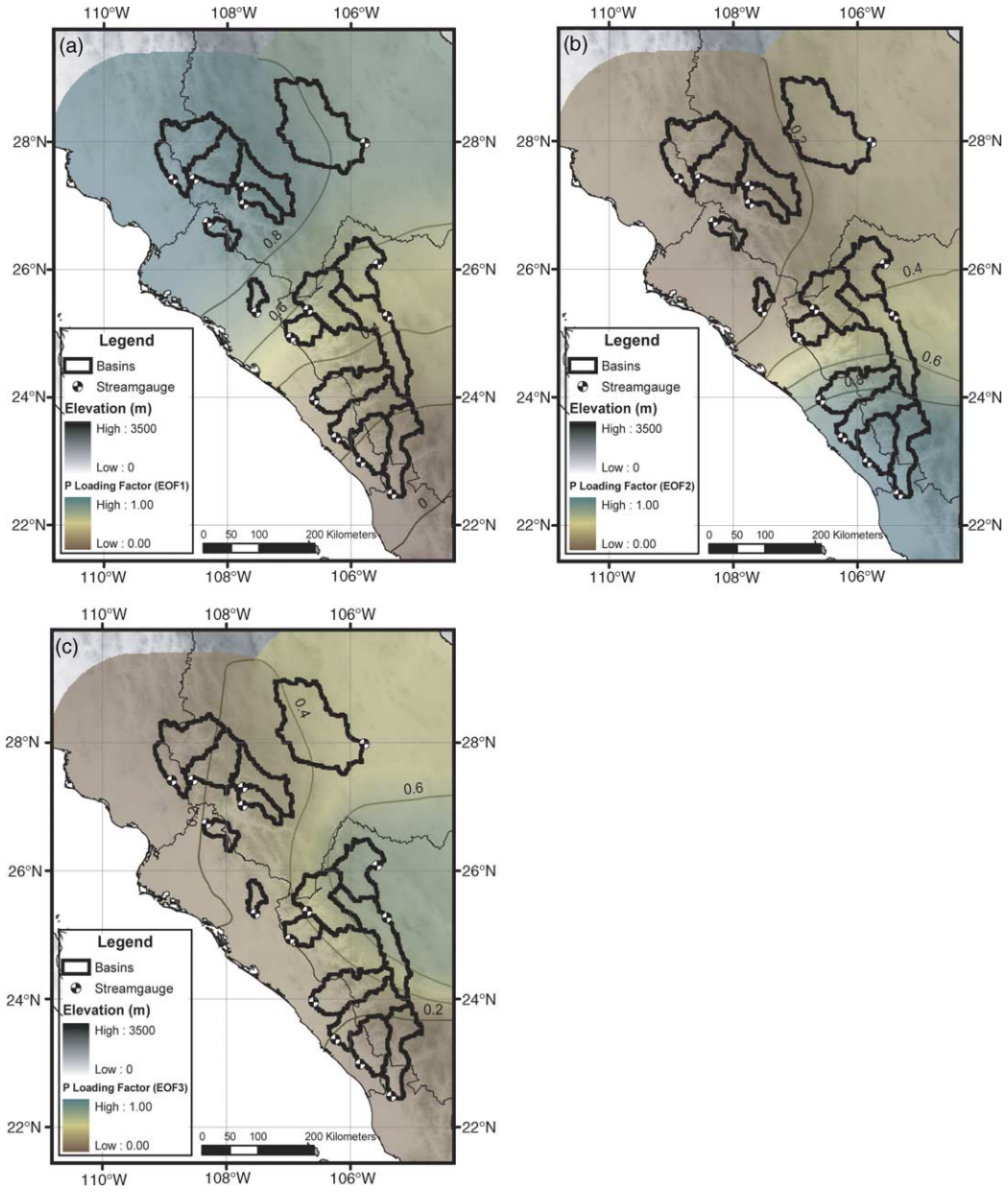

Fig. 4. Interpolated loading factors from PCA analysis of JAS basin-averaged precipitation for: (a) EOF1, (b) EOF2, and (c) EOF3. Contour interval is 0.2.

which explained 27.6% of the total variance) and an eastern region (EOF3—Fig. 4(c), which explained 13.4% of the total variance). A fourth coherent region (not shown), explaining 9.23% of the total variance, contained two (Tamazula, Badiraguato) of the three (third basin—Humaya) basins in the west-central region of the SMO. No similar grouping was found from the EOF analyses of streamflow. While this grouping is conceptually intriguing from the standpoint of precipitation character, study of its composite behavior is not pursued in the present work.

4.3. Monthly autocorrelation structure

Fig. 5 shows the 1-month lag autocorrelations for monthly flows in the 15 test basins. There is a clear annual signal in the autocorrelation values, with low flow months (Jan–Apr) tending to have strong serial correlations (0.5–0.97), indicating generally strong month-to-month persistence during the dry season. Autocorrelation values drop precipitously at the onset of the monsoon in response to large differences in monsoon onset dates from year to year. The onset of monsoon rains generally occurs during June and early July over most of the study region. Interannual variability in the onset of the monsoon therefore is the key factor influencing streamflow response in the early summer. There is not a strong recovery in the autocorrelation structure of streamflow until September–October. Instead, month-to-month correlation values remain low during July, August and September.

From Fig. 5, there is also some evidence suggesting that month-to-month persistence in warm-season streamflow may be regionally dependent. In particular, basins from EOF2 (dotted red lines, the southern region) tend to exhibit comparatively higher autocorrelation scores during Jun–Jul, Jul–Aug, Aug–Sep than do the other basins. This may be reflective of an increased frequency of precipitation and larger monthly totals compared to other regions, as shown by Gochis et al. (2004). Conversely, during Sep–Oct and Oct–Nov, the southern basins exhibit some of the lowest autocorrelation scores, even lower than those during the peak rainy months in many cases. This decrease in fall season autocorrelation values may be due to rare but important land-falling tropical storms onto the Mexican mainland (Englehart and Douglas, 2001).

4.4. Rainfall-runoff correlation structure

Brito-Castillo et al. (2003) showed a significant correlation structure using long-term, filtered time series of JAS precipitation and streamflow from NAM region. Here we focus not only on the seasonal correlation structure, but also on the monthly correlation structure in order to elucidate the evolution of precipitation-streamflow (P–Q) relationships during the NAM. The JAS and monthly P–Q Spearman rank correlation values for all 15 basins and for the three EOF composites are given in Table 2. Correlation values, significant at the 99% level, are shown in boldface. Each of the three EOF composites exhibits significant JAS correlations between streamflow and precipitation. The eastern slope region, EOF3, exhibits the highest JAS correlation value, followed by EOF1, the northern region, and EOF2, the southern region. In the individual basins comprising EOF2, JAS precipitation and streamflow are significantly correlated, although the correlation values are modest. This is not the case for all of the members of

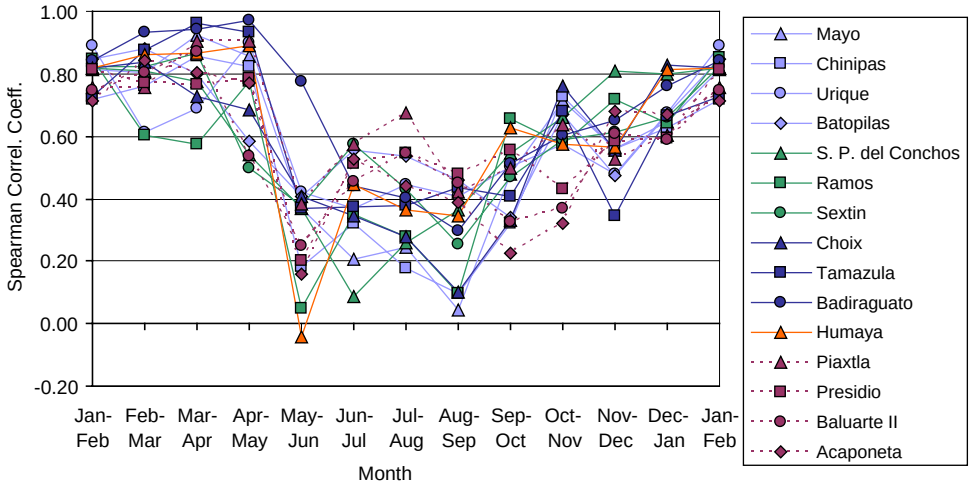

Fig. 5. Lag 1 ranked autocorrelation values for monthly streamflow volume anomalies.

Table 2
Spearman rank correlation scores (fraction) between streamflow and basin-averaged precipitation for 15 headwater basins and regional EOF composites in northwest Mexico

Basin	Area	*N*-pairs	JAS	Jul	Aug	Sep	Oct
1. San Pedro del Conchos	9405	41	**0.58**	0.35	**0.56**	**0.75**	0.32
2. Chinipas	5098	29	**0.49**	0.39	0.42	**0.69**	**0.70**
3. Mayo	7510	36	0.31	0.36	0.37	**0.55**	**0.68**
4. Urique	4000	27	0.37	0.06	0.27	**0.66**	**0.59**
5. Batopilas	2033	16	0.42	0.06	0.50	0.38	0.59
6. Choix	1403	39	**0.45**	0.31	0.34	**0.58**	**0.61**
7. Sextin	4911	21	**0.87**	**0.83**	0.50	**0.81**	0.38
8. Humaya	6149	29	0.42	0.28	**0.48**	**0.66**	**0.67**
9. Badiraguato	1018	40	0.23	0.23	0.24	**0.56**	**0.67**
10. Tamazula	2241	33	0.27	0.37	0.19	0.38	**0.57**
11. Ramos	7130	23	**0.92**	**0.70**	**0.60**	**0.85**	**0.53**
12. Piaxtla	6166	44	**0.42**	0.26	0.30	**0.59**	**0.49**
13. Presidio	5614	40	**0.56**	0.25	**0.45**	**0.73**	**0.60**
14. Baluarte	4635	48	**0.52**	**0.45**	**0.44**	**0.54**	**0.66**
15. Acaponeta	5092	49	**0.36**	**0.42**	**0.37**	**0.50**	**0.59**
EOF1 (North)		39	**0.56**	0.38	**0.51**	**0.64**	**0.70**
EOF2 (South)		50	**0.52**	0.28	**0.42**	**0.69**	**0.64**
EOF3 (East)		28	**0.79**	**0.56**	0.46	**0.71**	**0.65**

Correlation values significant and the 99.0% level shown in **bold**.

the EOF1 and EOF3 composites. In EOF3, the Sextin ($S=0.87$) and Ramos ($S=0.92$) basins yield rainfall-runoff correlation scores that are very high compared to other basins.

Monthly values of the composite *P–Q* correlation scores increase as the summer progresses. Neither EOF1 nor EOF2 are significantly correlated during the month of July, but are significantly correlated in August, September and October. (Similarly, the small low-elevation basins not grouped into the EOF composites, Choix, Badiraguato and Tamazula, do not exhibit significant *P–Q* correlations until Sept or Oct.) This pattern suggests that 'hydrological conditioning' of the watersheds, in terms of filling in-basin storages (e.g. soil moisture, depression and channel storages) is occurring. In effect, July rains in these basins contribute mostly to increasing soil moisture and filling depression and channel storages. Other potential factors affecting runoff response are higher potential evaporation rates during the early monsoon season or differing precipitation intensity, duration, and frequency characteristics, which could alter the partitioning of precipitation between infiltration and runoff. It may also be that local, shallow groundwater tables that feed ephemeral stream networks are not sufficiently recharged to promote sustained streamflows until later in the rainy season.

In contrast, EOF3 exhibits a minimum, and statistically insignificant, *P–Q* correlation scores during August. It is tempting to relate this to the regional mid-season summertime drought (or 'canicula', e.g. Magaña et al., 1999) that predominates over northeastern Mexico during July and August. However, the monthly, basin-averaged precipitation values from the gridded precipitation product actually peak during August for the Sextin, Ramos and Batopilas basins. As suggested earlier, deficiencies in the precipitation observing network along the eastern slope of the SMO may mask this and other subtle features in the regional precipitation regime.

Similar to the regional composites, monthly *P–Q* correlation scores from the individual basins generally increase from July through September or October. [The only basin, which exhibits no statistically significant *P–Q* score is the Batopilas basin. This is likely due to its short record and correspondingly small sample size ($N=16$).] Correlation scores for all basins, except the Sextin (an

eastside basin), peak in either September or October. Interestingly, total precipitation values for October are significantly less than in July, August or September for all basins. Therefore, the high correlation between rainfall and runoff in October (and to a lesser degree, September) reflects either a move of the partitioning of precipitation between evaporation, infiltration and runoff towards runoff production later in the summer and early fall, or the tendency for in-basin storages to have been filled by the end of the season.

With the exception of the limited study by Viramontes and Descroix (2003), the specific mechanisms for generating runoff from the SMO (e.g. infiltration excess, saturation excess or groundwater discharge) have yet to be clearly diagnosed. September and October are the peak months for land-falling tropical storms originating from the eastern Pacific (Englehart and Douglas, 2001). These storms can drop very large amounts of rain over one- to two-day periods, which would largely be converted into runoff. The climatological preference for these types of events to occur in September and October may also contribute to higher P–Q correlation scores during these months. No attempt is made in the present work to evaluate the impact of landfalling tropical storms on streamflow, but the authors believe that such a study would be quite fruitful.

4.5. Runoff coefficient structure

To examine the rainfall-runoff process further, seasonal and monthly runoff coefficient (Q_r) values were calculated for the composite regions and for individual basins. Regionalized JAS Q_r values (Table 3) range from 0.19 for EOF3, the eastern region, to 0.34 for EOF2, the southern region. The range in regionalized and individual basin monthly Q_r values from July to October is quite large and shows a clear regional behavior. Monthly Q_r values from EOF1, EOF2, and EOF3, range from 0.14 to 0.52, 0.22 to 1.02, and 0.11 to 0.32, respectively. The order of JAS and monthly Q_r values is physically plausible given that the southern basins receive the largest seasonal totals of precipitation, while the eastside basins typically receive the least amount of rain. In this semiarid setting, the drier the river basin, the less precipitation is partitioned into streamflow. Q_r values from EOF1, the northern SMO region, more closely resemble those of EOF3 than those of EOF2.

In each region, and in nearly all individual basins, Q_r values increase from July through October, which further illustrates the concept of hydrological

Table 3
As in Table 2 but for runoff coefficient values (fraction)

Basin	Area	JAS ($Q_r = Q/P$)	Jul	Aug	Sep	Oct
1. San Pedro del Conchos	9405	0.09	0.06	0.10	0.13	0.18
2. Chinipas	5098	0.27	0.19	0.30	0.35	0.75
3. Mayo	7510	0.18	0.12	0.22	0.26	0.55
4. Urique	4000	0.13	0.09	0.15	0.18	0.33
5. Batopilas	2033	0.22	0.18	0.25	0.22	0.43
6. Choix	1403	0.34	0.25	0.36	0.43	0.87
7. Sextin	4911	0.21	0.10	0.21	0.31	0.27
8. Humaya	6149	0.23	0.15	0.24	0.32	0.45
9. Badiraguato	1018	0.30	0.19	0.27	0.41	**1.18**
10. Tamazula	2241	0.40	0.32	0.42	0.53	**1.32**
11. Ramos	7130	0.15	0.08	0.16	0.19	0.26
12. Piaxtla	6166	0.33	0.21	0.34	0.47	**1.40**
13. Presidio	5614	0.24	0.15	0.23	0.36	0.63
14. Baluarte	4635	0.43	0.28	0.43	0.64	**1.23**
15. Acaponeta	5092	0.34	0.22	0.32	0.48	0.81
EOF1 (North)		0.21	0.14	0.23	0.29	0.52
EOF2 (South)		0.34	0.22	0.33	0.49	**1.02**
EOF3 (East)		0.19	0.11	0.20	0.25	0.32

Values in **bold** indicate runoff coefficients greater than 1.0.

conditioning. July Q_r values range from 6 to 32% with the eastside basin values (Sextin, Ramos and San Pedro del Conchos) less than or equal to 10%. By October, Q_r values range from 18 to 140%. The southern region, EOF2, possesses October Q_r values greater than 100% indicating that more water is being discharged from the basin as streamflow than is falling as precipitation. Hence, while rainfall and runoff may be well correlated in October, it is apparent that many basins are beginning to empty from their peak 'conditioned' state.

5. Summary and conclusions

This study presents a regional hydroclimatology of 15 headwater catchments that drain the Sierra Madre Occidental mountains in northwest Mexico. The basins range in size from 1000 to 10,000 km^2 and are unregulated to the best of the authors' knowledge. Hence, this analysis is aimed at elucidating the natural streamflow response of headwater catchments from the annual cycle of precipitation in northwest Mexico, which is generally dominated by a warm-season monsoon. This study fills a niche in previous research in this region that has predominantly focused on smaller basin-scale processes (e.g. Descroix et al., 2002a,b; Viramontes and Descroix, 2003), global-scale analyses (e.g. Dettinger and Diaz, 2000) or the inter-annual variability of streamflow and precipiation Brtio-Castillo et al. (2002; 2003). While similar, in nature to the regional analyses of Brito-Castillo et al. (2002; 2003), this study presents a more detailed description of the annual cycle of streamflow as well as the intra-seasonal evolution of rainfall-runoff relationships during the summer monsoon season. The principal findings from this study can be summarized as follows:

- Across northwestern Mexico, the natural streamflow regime is dominated by warm season rainfall associated with the NAM system. In the 15 headwater catchments studied, streamflow volume during July, August and September constituted between 50 and 85% of the total annual streamflow. A secondary, though much smaller, maximum in monthly streamflow values was observed in the early winter along catchments draining the western slope of the Sierra Madre. This secondary maximum is likely due to infrequent baroclininc disturbances.
- Monthly coefficients of streamflow variability are lowest during the peak streamflow months of JAS and range between 40 and 150% for all basins. While this implies that standard deviations in monthly streamflow are low compared to the mean values, the magnitude of these deviations can be substantial fractions of the mean annual flow volume and, thus, can be critically important for the management of regional water resources. Monthly coefficients of variation in all other months range between 75 and 350% of monthly mean values. The importance of this higher degree of variability in non-peak months may appear to be diminished by the values of the standard deviations in these months comprising much smaller fractions of mean annual streamflow. However, winter precipitation can be critical for averting water shortages during the late winter and spring irrigation seasons across northwest Mexico.
- Streamflow maxima for the periods of record appear to show some regional dependence. Basins draining the eastern slope of the SMO uniformly have their record streamflow months during either August or September. Basins draining the western SMO tend to receive their record streamflow months either during August–September or December–January.
- The autocorrelation structure of monthly streamflow volumes also shows a distinct annual cycle, which contains the lowest month-to-month correlation values, both at the onset of, and throughout, the summer monsoon season. Autocorrelation values outside of the monsoon season are comparatively higher, indicating strong month-to-month persistence during the dry season. There is some evidence that streamflow persistence during the peak monsoon months is strongest in the southernmost basins (EOF2) but that month-to-month persistence in these basins decays during autumn.
- A Varimax Rotated EOF analysis of seasonal (JAS) streamflow revealed three distinct regions of coherent streamflow variability: a northern region (EOF1), a southern region (EOF2), and an eastern region (EOF3). The three EOF's explain

approximately 71% of the JAS inter-annual streamflow variability. An identical analysis performed on a long-term gridded precipitation data set revealed a similar set of three regions of coherent precipitation variability, which explained approximately 86% of the JAS precipitation variability.

- Precipitation-streamflow (P–Q) relationships as diagnosed by both rank correlation scores between monthly and seasonal precipitation and streamflow as well as monthly and seasonal runoff coefficients showed a strong regional behavior that corresponded well to the three regions defined by the EOF analyses. Seasonal P–Q correlations tended to be highest for eastern-slope basins, followed by basins in the southwestern SMO, then by those draining the northwestern SMO. Regional composites and individual basin P–Q values tended to increase from July through October. Basins along the eastern SMO did not clearly exhibit this seasonal increase. Smaller catchments along the western slope of the SMO generally did not possess statistically significant correlation values until September or October.
- Over the course of a warm season (JAS), averages of approximately 21, 34 and 19% of rainfall was converted to streamflow for the northern, southern and eastern regions, respectively. Early season (July) values of the runoff coefficient ranged from 6 to 32%. By October, values ranged between 18 and 140%. Runoff coefficients were highest in the southern region where rainfall was highest. In nearly all basins and composite regions, runoff coefficient values increased from July through October, indicating the process of hydrological conditioning. Runoff coefficient values exceeding 100% occurred in 4 of the 15 basins during October, which indicates basin discharge exceeding rainfall as summer rains decrease.

This study shows the strong dependence of streamflow and, therefore, water resources, on monsoon rains. While the monsoon rains are, generally, a stable feature of the warm season climate in western Mexico, variability in the onset and total amounts of rainfall can have a significant impact on the annual water resource budget. In addition to the peak streamflow generation period between July and October, autumnal land-falling tropical storms and cool season baroclinic disturbances can generate significant amounts of streamflow. As evidenced by high coefficients of variation outside the peak monsoon season, these events tend to be infrequent and therefore not particularly dependable for water resources planning. Attempts to correlate the occurrence of wintertime streamflow with large-scale teleconnection mechanisms such as the ENSO or the PDO have revealed only transient correlations that are not robust over long periods (e.g. Brito-Castillo et al., 2002).

There are several shortcomings of this current study that require address. The first is that the streamflow records used do not perfectly overlap. There are missing months in many of the streamflow records and several gages have differing periods of record. Most of the streamflow data are fairly complete from the 1970s through the mid 1990s. Prior to 1970, however, there are progressively fewer station records. Differences in streamflow records can present difficulties when looking at regional variability characteristics, due to missing data points within different basins. Missing data points can also be very important in the identification of record streamflow events, which can possibly go unobserved. Despite the incompleteness of the streamflow record used here, the regional behavior of many of the streamflow characteristics and rainfall-runoff relationships are consistent with known regional precipitation patterns, suggesting that the principal features of the overall streamflow regime are well captured.

One of the most significant sources of uncertainty in this study is the gridded precipitation dataset. The cooperative observer network in Mexico provided the majority of the data used to create the gridded analyses. Given the sparse population in and along the flanks of the SMO, there is a corresponding paucity of observation points. Interpolated values at a specific location can be heavily or completely influenced by surrounding data points that may be several 10's to 100's of kilometers away. This discrepancy can result in significant local and regional biases in estimated precipitation. Given this potential source of error, it was not possible to examine, with confidence, the relationship between precipitation characteristics, such as intensity thresholds or frequency, and streamflow. For example, on a given

day during the monsoon, nearly all gridpoints within the analysis domain possess non-zero values of precipitation as a result of a smoothing filter applied during the modified Cressman analysis. It is therefore problematic to perform a traditional 'wet-day' analysis, and instead one must choose a precipitation threshold with which to recognize 'wet-days'. Hence, analysis of higher order precipitation characteristics and their relationship to streamflow, as suggested by Gochis et al. (2003a), is currently prohibited.

Notwithstanding these shortcomings, there is a clear seasonality and regionality to the hydroclimatological regime in Northwest Mexico. While this study presents some general features of this regime and some of the regional patterns of streamflow variability, detailed examination of rainfall runoff processes on a region-wide basis will remain dependent upon an upgraded regional hydrometeorological observing network. Part of this upgrade has begun under the auspices of the NAME in the form of a new automated raingage network within the SMO (Gochis et al., 2003b; 2004) as well as recent installations of automatic weather stations by the Servicio Meteorologico Nacional of Mexico. Data from this enhanced raingage network, as well as other instruments to be deployed as part of the NAME field campaign during the summer of 2004, should provide a much improved representation of precipitation, which will subsequently be used in both the diagnostic and modeling studies to improve both understanding and prediction of streamflow in this water-stressed region.

Acknowledgements

The authors wish to thank Subrhendu Gangopadhyay for his insightful advice on interpreting the principal components analysis, the Comision Nacional del Agua of Mexico for collecting and providing the streamflow data used in this work, to Dr Tom Warner for his helpful review of this article and to two anonymous reviewers whose generous feedback greatly improved the quality and clarity of this work. Support for this work is provided by the National Center for Atmospheric Research, NOAA Office of Global Programs grant numbers NA16GP2002 and NA030AR4310073 and by Mexico CONACYT grant ZAC-2004-C01-0030.

References

Anderson, B.T., Roads, J.O., Chen, S.C., Juang, H.-M., 2000. Regional similation of the low-level winds over the ulf of California and southwestern United States. J. Geophys. Res. 105 (D14), 17955–17969.

BANDAS, 1998. Bancos Nacional de Datos de Aguas Superficiales, Comission Nacional del Agua (CNA) y Instituto Mexicano de Tecnologia del Agua (IMTA), CD-ROM.

Berbery, E.H., 2001. Mesoscale moisture analysis of the North American Monsoon. J. Climate 14, 121–137.

Brito-Castillo, L., Leyva-Contreras, A., Shelutko, V.A., 1999. Determination of decadal climatic cycle in runoff fluctuation of a hydrologic unit. Atmosfera 11, 27–42.

Brito-Castillo, L., Leyva-Contreras, A., Douglas, A.V., Lluch-Belda, D., 2002. Pacific-decadal oscillation and the filled capacity of dams on the rivers of the gulf of California continental watershed. Atmosfera 15, 121–138.

Brito-Castillo, L., Douglas, A.V., Layva-Contreras, A., Lluch-Belda, D., 2003. The effect of large-scale circulation on precipitation and streamflow in the gulf of California continental watershed. Int. J. Climatology 23, 751–768.

Carleton, A.M., Carpenter, D.A., Webster, P.J., 1990. Mechanisms of interannual variability of the southwest United States summer rainfall maximum. J. Climate 3, 999–1015.

Castro, C.L., McKee, T.B., Pielke Sr.., R.A., 2001. The relationship of the North American monsoon to tropical and North Pacific sea surface temperatures as revealed by observations analyses. J. Climate 14, 4449–4473.

Comrie, A.C., Glenn, E.C., 1998. Principal components-based regionalization of precipitation regimes across the southwest United States and northern Mexico, with an application to monsoon precipitation variability. Climate Res. 10, 201–215.

Cressman, G.P., 1959. An operational objective analysis system. Mon. Wea. Rev. 87, 367–374.

Descroix, L., Nouvelot, J.F., Vauclin, M., 2002a. Evaluation of an antecedent precipitation index to model runoff yield in the western sierra madre (Northwest Mexico). J. Hydrol. 263, 114–130.

Descroix, L., Gonzalez-Barrios, J.L., Vanervaere, J.P., Viramontes, D., Bollery, A., 2002b. An experimental analysis of hydrodynamic behavior on soil and hillslopes in a subtropical mountainous environment (western Sierra Madre, Mexico). J. Hydrol. 266, 1–14.

Dettinger, M.D., Diaz, H.F., 2000. Global characteristics of streamflow seasonality and variability. J. Hydromet. 1 (4), 289–310.

Douglas, A.V., 2000. The influence of eastern North Pacific tropical storms on summer rainfall in Mexico, Second Southwest Wea. Symposium September (Tucson, AZ), pp. 21–22.

Douglas, M., Maddox, R.A., Howard, K., Reyes, S., 1993. The Mexican monsoon. J. Climate 6, 1665–1677.

Englehart, P.J., Douglas, A.V., 2001. The role of eastern North Pacific tropical storms in the rainfall climatology of western Mexico. Int. J. Climatology 21, 1357–1370.

Englehart, P.J., Douglas, A.V., 2002. Mexico's summer rainfall patterns: an analysis of regional modes and changes in their teleconnectivity. Atmosfera 15, 147–164.

ESRI, 2003. ArcMap Version 8.2. Environmental Systems Research Institute, Inc.

Fawcett, P.J., Stalker, J.R., Gutzler, D.S., 2002. Multistage moisture transport into the interior of northern Mexico during the North American summer monsoon. Geophys. Res. Lett. 29 (23) (Art. No. 2094).

Fuller, R.D., Stensrud, D.J., 2000. The relationship between tropical easterly waves and surges over the gulf of California during the North American monsoon. Mon. Wea. Rev. 128 (8), 2983–2989.

Gochis, D.J., Shuttleworth, W.J., Yang, Z.-L., 2003a. The hydrometeorological response of the modeled North American monsoon to convective parameterization. J. Hydromet. 4, 235–250.

Gochis, D.J., Leal, J.-C., Watts, C.J., Shuttleworth, W.J., Garatuza-Payan, J., 2003b. Preliminary diagnostics from an event based precipitation observation network in support of the North American monsoon experiment (NAME). J. Hydromet. 4 (5), 974–981.

Gochis, D.J., Leal, J.-C., Jimenez, A., Watts, C.J., Garatuza-Payan, J., Shuttleworth, W.J., 2004. Analyses of 2002 and 2003 North American monsoon precipitation form the NAME event raingauge network (NERN). Mon. Wea. Rev. 132, 2938–2953.

Higgins, R.W., Shi, W., 2000. Dominant factors responsible for interannual variability of the summer monsoon in the southwestern United States. J. Climate 13, 759–776.

Higgins, R.W., Shi, W., 2001. Intercomparison of the principal modes of interannual and intraseasonal variability of the North American monsoon system. J. Climate 14 (3), 403–417.

Higgins, R.W., Janowiak, J.E., Yao, Y., 1996. A gridded hourly precipitation data base for the United States (1963–1993). NCEP/Climate Prediction Center ATLAS 1, p. 47.

Higgins, R.W., Yao, Y., Wang, X., 1997. Influence of the North American monsoon system on the United States summer precipitation regime. J. Climate 10, 2600–2622.

Higgins, R.W., Mo, K.C., Yao, Y., 1998. Interannual variability of the United States summer precipitaion regime with emphasis on the southwestern monsoon. J. Climate 11, 2582–2606.

Higgins, R.W., Chen, Y., Douglas, A.V., 1999. Interannual variability of the North American warm season precipitation regime. J. Climate 12, 653–680.

Higgins, R.W., Douglas, A., Hahmann, A., Berbery, E.H., Gutzler, D., Shuttleworth, J., Stensrud, D., Amador, J., Carbone, R., Cortez, M., Douglas, M., Lobato, R., Meitin, J., Ropelewski, C., Schemm, J., Schubert, S., Zhang, C.D., 2003. Progress in pan American CLIVAR research: the North American monsoon system. Atmosfera 16 (1), 29–65.

Hu, Q., Feng, S., 2002. Interannual rainfall variations in the North American summer monsoon region: 1900–1998. J. Climate 15, 1189–1202.

INEGI, 1993. Estudio hidrologico del estado de sonora, Instituto Nacional Estadistica, Geografia e Informatica. Aguascalientes, Ags., Mexico, p. 185.

INEGI, 1995. Esutio Hidrologico del Estado de Sinaloa. Instituto Nacional Estadistica, Geografia e Informatica. Aguascalientes, Ags., Mexico, p. 88

Magaña, V.O., 1999. Los Impactos de El Nino en Mexico, p. 229.

Magaña, V.O., Conde, C., 2000. Climate and freshwater resources in northern Mexico: Sonora, a case study. Env. Monit. Assess 61, 167–185.

Magaña, V.O., Amador, J., Medina, S., 1999. The midsummer drought over Mexico and central America. J. Climate 12, 1577–1588.

Michaud, J.D., Hirschboeck, K.K., Winchell, M., 2000. Regional variations in small-basin floods in the United States. Water Resour. Res. 37 (5), 1405–1416.

Mo, K.C., Juang, H.M.H., 2003. Influence of sea surface temperature anomalies in the Gulf of California on North American monsoon rainfall. J. Geophys. Res. 108 (D3), 4112. doi:10.1029/2002/JD002403.

Mo, K.C., Peagle, J.N., 2000. Influence of sea surface temperature anomalies on the precipitation regimes over the Southwest United States. J. Climate 13 (20), 3588–3598.

Mosino, P., Garcia, E., 1974. The climate of Mexico. World survey of climatology. In: Bryson, R.A., Hare, K.F. (Eds.), Climates of North America, vol. 11. Elsevier, pp. 345–404.

NAME Science Working Group, cited 2004: North American Monsoon Experiment (NAME) Science and implementation plan. [Available online at http://www.cpc.ncep.noaa.gov/products/precip/monsoon/NAME.html].

Negri, A.N., Adler, R.F., Nelkin, E.J., Huffman, G.J., 1994. Regional rainfall climatology derived from special sensor microwave imager (SSM/I) data. Bull. Am. Met. Soc. 75 (7), 1165–1182.

North, G.R., Bell, T.L., Cahalan, R.F., 1982. Sampling errors in the estimation of empirical orthogonal functions. Mon. Wea. Rev. 110, 699–706.

Schmitz, J.T., Mullen, S.L., 1996. Water vapor transport with the summertime North American monsoon as depicted by ECMWF analysis. J. Climate 9, 1621–1634.

Stensrud, D.J., Gall, R.L., Mullen, S.L., Howard, K.W., 1995. Model climatology of the Mexican monsoon. J. Climate 8, 1775–1794.

Vazquez, M.C., 1999. Annual cycle of convective activity in Mexico. Atmosfera 12 (2), 101–110.

Viramontes, D., Descroix, L., 2003. Changes in the surface water hydrologica characteristics of an endoreic basin of northern Mexico from 1970 to 1998. Hyd. Proc. 17, 1291–1306.